

scientific data

OPEN
DATA DESCRIPTOR



Multiaxial vibration data for blade fault diagnosis in multirotor unmanned aerial vehicles

Luttfi A. Al-Haddad¹✉, Alaa Abdulhady Jaber¹, Mohsin N. Hamzah¹, Habib Kraiem²✉, Mustafa I. Al-Karkhi¹ & Aymen Flah^{3,4,5}

This dataset presents multiaxial vibration signals collected from a multirotor unmanned aerial vehicle (UAV) operating in hover mode for the purpose of blade fault diagnosis. Vibration measurements were recorded at the geometric center of the UAV, where the centerlines of the four rotor arms intersect, using a triaxial accelerometer. The dataset captures variations across the X, Y, and Z axes under different blade fault conditions, including healthy, minor imbalance, severe imbalance, and screw loosening scenarios. Each flight scenario was repeated under controlled conditions to ensure consistency and high-quality labeling. The resulting soft-labeled dataset includes time-domain signals from numerous test flights and has been used in multiple prior studies involving classical and deep learning-based fault classification techniques. This curated data collection provides a valuable resource for researchers in UAV health monitoring, vibration analysis, and machine learning-based fault diagnosis. The dataset is particularly useful for the development and benchmarking of signal processing pipelines and classification models aimed at identifying blade-level faults in multirotor UAV systems.

Background & Summary

Unmanned aerial vehicles (UAVs) are increasingly integrated into modern applications across diverse fields, including logistics¹, surveillance², research³, and recreation⁴. As UAV deployment scales, the importance of real-time fault diagnosis systems grows in parallel to ensure operational safety in work efficiency and general reliability⁵⁻⁸. Among the various components vulnerable to malfunction, propeller blades are particularly critical; their imbalances or structural anomalies can cause flight instability or failure. Vibration-based monitoring, especially when paired with Artificial Intelligence (AI) intelligent algorithms, offers a promising approach to identify such faults preemptively. With the advancement of onboard sensing, data acquisition, and AI-enabled processing, the development and public availability of curated vibration datasets is essential to accelerate research and standardize evaluation in UAV health diagnostics.

The dataset described in this paper has been extensively utilized in previously published works. In the first study, a structured protocol for UAV fault diagnosis was developed, where the dataset was used to demonstrate the workflow for collecting, preprocessing, and analyzing vibration signals through machine learning (ML)⁹. In the second study, multi-resolution transform features were extracted and fed into a deep neural network for fault classification¹⁰. In the third, an unbalance classification method was implemented using an optimized stochastic gradient descent logistic regression model¹¹. In the fourth study, feature selection using the Relieff method was applied prior to fault classification using variant ML models, namely SVM and kNN models¹². In the fifth, signal filtering was compared with multiresolution analysis methods to assess their performance in fault detection¹³. In the sixth, finite element analysis was conducted alongside experimental validation using the dataset to study the impact of consumed propellers on UAV airworthiness¹⁴. In the seventh study, frequency-domain vibration signal analysis was applied on the dataset's time-domain signals to classify unbalance faults¹⁵. Finally, in the eighth study, discrete wavelet and fast Fourier transforms were combined to enhance signal decomposition and

¹Mechanical Engineering Department, University of Technology- Iraq, Baghdad, Iraq. ²Center for Scientific Research and Entrepreneurship, Northern Border University, Arar, 73213, Saudi Arabia. ³University of Business and Technology (UBT), College of Engineering, Jeddah, 21448, Saudi Arabia. ⁴Applied Science Research Center, Applied Science Private University, Amman, 11931, Jordan. ⁵ENET Centre, CEET, VSB-Technical University of Ostrava, Ostrava, Czech Republic. ✉e-mail: Luttfi.a.alhaddad@uotechnology.edu.iq; ALhabeeb.Kareem@nbu.edu.sa

Ref.	Dataset Used	Methodology	Approach	Evaluation Criteria
⁹	Multiaxial Vibration Signals at UAV Center with Blade Faults (MVS-UAV-BF)	Protocol-based data collection and ML framework	Both (Signal Processing + ML)	Workflow protocol description
¹⁰	MVS-UAV-BF	Multi-resolution features + DNN	AI (ML – DNN)	Classification Accuracy
¹¹	MVS-UAV-BF	Logistic Regression with SGD optimization	AI (ML – OSGD-LR)	Accuracy
¹²	MVS-UAV-BF	ReliefF feature selection + SVM/kNN	AI (ML – SVM, kNN)	Accuracy, Processing Time
¹³	MVS-UAV-BF	Kalman Filtering & Wavelet Transform	Signal Processing	Fault detection performance
¹⁴	MVS-UAV-BF	Finite Element + Experimental Validation	Signal Processing	Modal/Natural Frequency Matching
¹⁵	MVS-UAV-BF	Frequency-domain analysis + Classification	Both	Fault Classification
¹⁶	MVS-UAV-BF	DWT + FFT fusion	Signal Processing	Fault Identification Resolution

Table 1. Summary of prior studies using the dataset.

Parameter	Value
Takeoff Weight	249 g
Max Flight Time	31 minutes
Max Hover Time	29 minutes
Max Flight Speed	16 m/s
GNSS	GPS + GLONASS + Galileo
Max Altitude	4000 m above sea level
Dimensions (Folded)	138 × 81 × 58 mm
Rotor Configuration	4 rotors (quadcopter)

Table 2. Specifications of the DJI Mini 2 Combo UAV.

improve fault identification¹⁶. The diverse applications and methodologies employed across these studies are summarized in Table 1.

This repeated application across eight peer-reviewed studies highlights the dataset's robustness, consistency, and value across different domains. This ranged from purely analytical signal transformations to advanced AI-based deep learning classifiers. The dataset is particularly effective in capturing and distinguishing multiaxial vibration responses of multirotor UAVs under various propeller fault conditions which makes it a versatile and reusable resource for researchers, educators, and developers of embedded health monitoring systems. Its availability encourages continued experimentation, benchmarking, and innovation in UAV fault diagnosis. In prior studies utilizing this dataset, both time-domain statistical features (e.g., RMS, standard deviation) and frequency-domain features derived from FFT or wavelet transforms have been used for fault classification. The dataset's proven utility across multiple published studies ensures it can serve as a foundation for future advancements in the field.

Recent advancements in UAV diagnostics have highlighted the benefits of incorporating richer sensor modalities, real-time processing, and embedded implementations. For instance, Kim *et al.* demonstrated effective fault localization and severity estimation in multicopters using accelerometer and gyroscope data with PCA and ANN/SVM models¹⁷. Yaman *et al.* proposed an embedded SVM-based fault detection method optimized for low-cost onboard implementation¹⁸, while Baldini *et al.* employed vibration analysis to enable real-time propeller fault detection under operational conditions¹⁹. In a more hardware-centric approach, Sadhu *et al.* implemented onboard deep learning fault classification using FPGA-based systems for real-time diagnosis²⁰. Additionally, the predictive scope of UAV reliability has been extended to battery performance, as shown by Al-Haddad *et al.*, who utilized deep neural networks for forecasting energy consumption and efficiency degradation trends in UAV power systems²¹. Collectively, these works underscore the relevance of curated datasets like ours, which provide high-quality, reusable vibration data that can serve as a diagnostic benchmark, simulation input, or model training foundation within a rapidly evolving UAV research landscape.

Methods

This section is to detail the adopted methodology, the used tools, and the experimental setup for the acquired dataset.

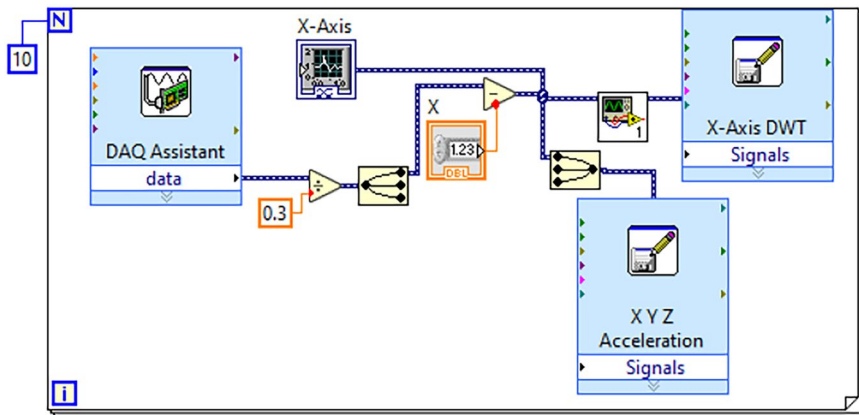
UAV model and tools. In this study, a DJI Mini 2 Combo quadcopter was used as the aerial platform for vibration data collection. This compact UAV offers reliable stability in hover mode and is suitable for replicable laboratory experiments. The key specifications of the UAV are listed in Table 2.

To capture the vibration signals, an ADXL335 triaxial analog accelerometer was mounted at the geometric center of the UAV—specifically at the point where the four motor arms intersect. This placement allows equal sensitivity to all axis-aligned vibrations resulting from blade imbalances. The ADXL335's specifications are provided in Table 3.

Parameter	Value
Axes	X, Y, Z
Output Type	Analog
Measurement Range	$\pm 3\text{ g}$
Sensitivity	300 mV/g (typical)
Power Supply	1.8 V to 3.6 V
Operating Temperature	-40 °C to +85 °C
Bandwidth (typical)	1600 Hz

Table 3. Specifications of the ADXL335 accelerometer.

Parameter	Value
Analog Inputs	8 channels (12-bit)
Sample Rate	10 kS/s (max)
Analog Output	2 channels (8-bit)
Digital I/O	12 lines
Communication	USB 2.0
Software Compatibility	LabVIEW, MATLAB, etc

Table 4. Specifications of the NI USB-6008 Data Acquisition System.**Fig. 1** LabVIEW block diagram used for real-time signal calibration.

The accelerometer was interfaced with a National Instruments DAQ-6008 USB data acquisition device, which relayed signals to the PC. Specifications of the DAQ system are shown in Table 4.

Sensor calibration was carried out by subtracting the mean from each raw signal in a continuous loop within LabVIEW. This eliminated initial signal drift and ensured zero-centered vibration recordings. The calibration method ensured smooth acquisition and alignment across all three axes. The LabVIEW block diagram representing this calibration logic is illustrated in Fig. 1.

It is noted that only external accelerometer data are included in this dataset, while onboard gyroscope and magnetometer readings were intentionally excluded to maintain a focused scope on time-domain vibration signals suitable for frequency-domain and time-frequency domain transformations.

Fault initiation and flight conditions. All vibration recordings were acquired while the UAV operated in hover mode at a fixed altitude of 1.2 meters. Two primary fault types were introduced to simulate propeller-level imbalances:

- Mass Removal Fault: A small section of the blade was trimmed to simulate mechanical wear or damage.
- Weight Unbalance Fault: Small adhesive sticky tape was affixed to one side of a blade to induce mass asymmetry.

Each type of fault was implemented independently on individual blades. For reference, blade numbering follows a clockwise pattern as viewed from above: Blade 1 (lower right), Blade 2 (upper right), Blade 3 (upper left), and Blade 4 (lower left). The fault configurations and blade numbering scheme are presented in Fig. 2.

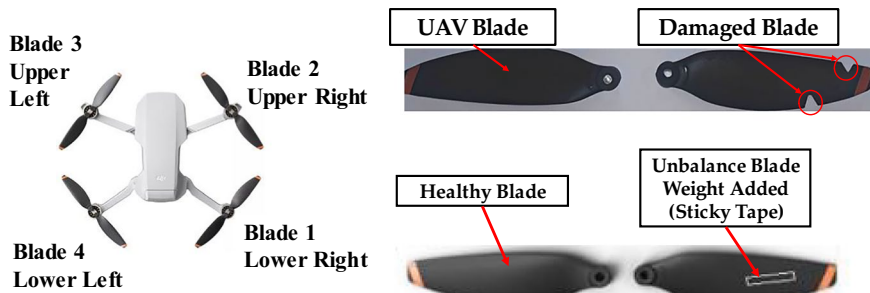


Fig. 2 Blade numbering and fault application methods (mass removal and weight unbalance).

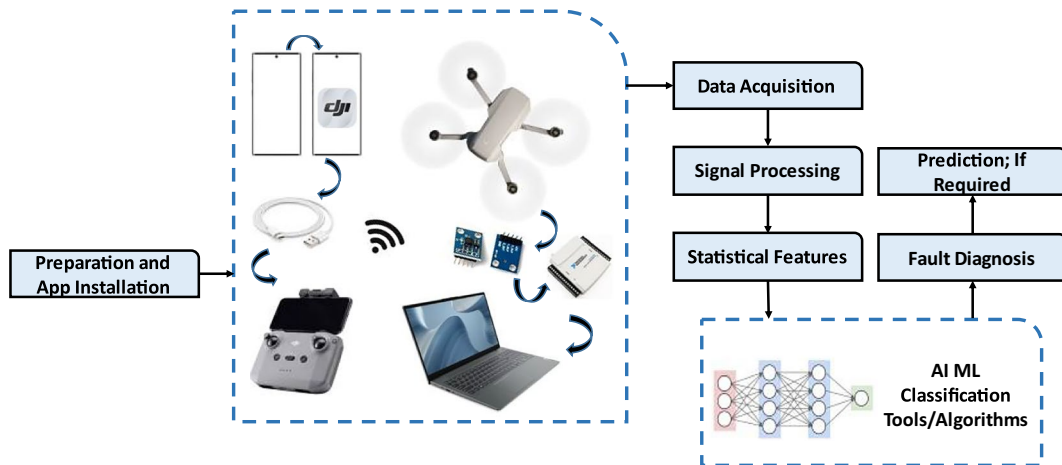


Fig. 3 Graphical methodology outlining the data acquisition and preprocessing workflow.

Each flight session lasted 7 minutes (420 seconds), during which approximately 400,000 vibration samples were collected per case. All experiments were conducted indoors in a controlled environment with no wind interference and stable room temperature, ensuring consistency and high-quality data across recordings.

This dataset is limited to a single UAV model operated at a fixed altitude under windless indoor conditions, which should be considered when evaluating its applicability to real-world scenarios. It is also acknowledged that the dataset is limited to hover-mode data collected in a controlled indoor setting, and future versions may incorporate dynamic flight conditions and environmental variations to enhance real-world applicability.

Control input data such as roll, pitch, and thrust commands were not recorded in this study, as the UAV was operated in a steady hover mode with minimal control variation; however, their integration will be explored in future datasets involving dynamic flight conditions.

Data acquisition and preprocessing. The full experimental workflow is summarized in Fig. 3, which shows the step-by-step process from UAV flight setup and sensor mounting to data recording, labeling, and storage.

The actual experimental setup including the UAV, DAQ system, sensors, and PC platform is visually represented in Fig. 4.

Vibration signals were recorded directly in the time domain and stored as Excel (.xlsx) files on the PC platform. To ensure usability and clarity, each signal file was manually labeled by the experimenter, indicating the type and location of the fault. For each flight condition—healthy, mass removal on one blade, and weight unbalance on another—recordings were repeated five times, resulting in a comprehensive and reliable dataset spanning five healthy and five faulty scenarios.

Data Records

The dataset is available at Figshare²². The complete dataset consists of five Excel files, each corresponding to a specific flight condition of the UAV, including both healthy and faulty cases. These cases involve controlled modifications to the UAV's propeller blades, such as mass removal (to simulate damage) and weight addition using adhesive tape (to induce imbalance). The dataset was collected under repeatable indoor hover flight

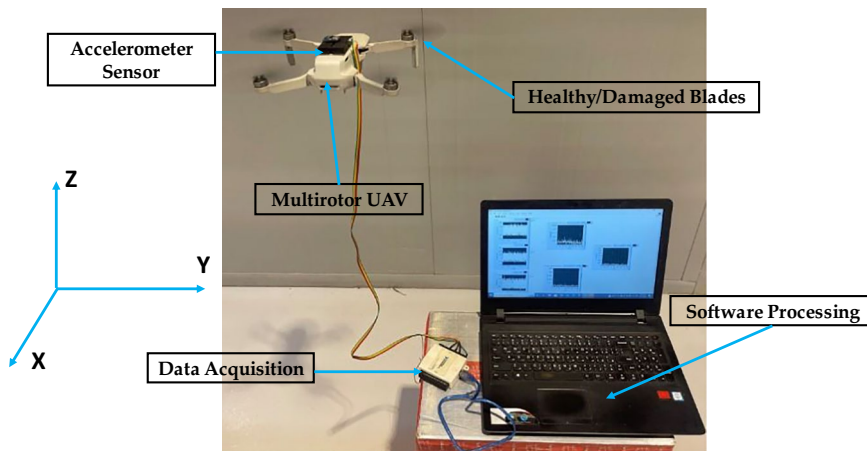


Fig. 4 Experimental setup showing the UAV, DAQ device, accelerometer, and PC platform.

First column: Time domain in seconds, Second column: X-axis vibrations, Third column: Y-axis vibrations, and Fourth column Z-axis vibrations.

Name

- Damaged Bottom Right Blade
- Damaged Top Right Blade
- Healthy
- Unbalanced Bottom Right Blade
- Unbalanced Top Right Blade

	A	B	C	D
1	Time (s)	X Acceleration	Y Acceleration	Z Acceleration
2	0.000977	-0.491271	-0.070494	-0.152043
3	0.001953	-0.253358	0.090947	-0.305018
4	0.00293	0.273451	0.235394	0.272888
5	0.003906	0.451886	0.158922	0.017929
6	0.004883	0.222469	0.328859	0.340877

Data starts from row 1 to around row 400,000 with the same instances of m/s^2 vibration signals

	A	B	C	D
399995	421.511286	0.061028	-0.316904	-0.007566
399996	421.512262	-0.049432	-0.444357	-0.135046
399997	421.513239	-0.397805	-0.036507	-0.126547
399998	421.514215	-0.185382	0.60076	-0.007566
399999	421.515192	0.154494	0.609256	0.238894
400000	421.516168	0.315935	-0.095985	0.162406

Data file contains five excel files

Fig. 5 Structure and contents of the dataset files. Each Excel file includes vibration data recorded across the X, Y, and Z axes, sampled over 400,000 instances per flight condition.

conditions, using a centrally mounted ADXL335 triaxial accelerometer connected to a NI USB-6008 DAQ system, as described in Section 3. Each file contains approximately 400,000 rows of raw, high-resolution vibration signals recorded continuously over a 7-minute period. The files are named clearly to reflect the specific fault case they represent:

- Healthy
- Damaged Bottom Right Blade
- Damaged Top Right Blade
- Unbalanced Bottom Right Blade
- Unbalanced Top Right Blade

Each Excel file includes four columns, structured as follows:

- Column A: Time (in seconds)
- Column B: X-axis acceleration (m/s^2)
- Column C: Y-axis acceleration (m/s^2)
- Column D: Z-axis acceleration (m/s^2)

Manual labeling was used to ensure maximum clarity, with filenames explicitly indicating the fault condition and blade position. All data are recorded in the time domain, suitable for transformation into frequency or

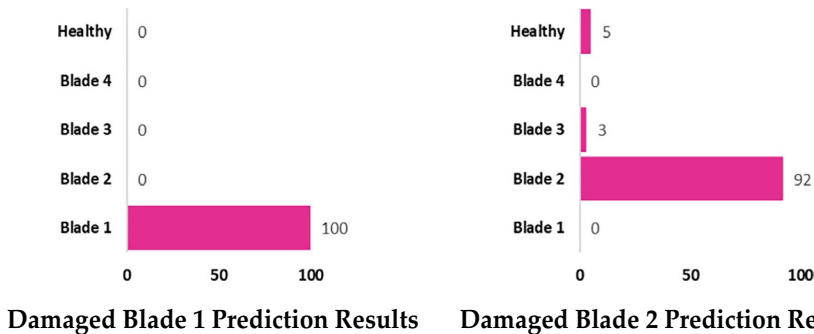


Fig. 6 Classification results of unseen damaged blade instances using pre-trained ML models.

time-frequency domains depending on user needs. These characteristics make the dataset especially useful for UAV diagnostics, machine learning classification tasks, and vibration signal analysis. Figure 5 details the data records.

Technical Validation

To ensure the reliability, quality, and scientific usability of the presented vibration dataset, two independent validation techniques were employed. These methods served to verify the clarity of the signal response, confirm accurate labeling, and assess noise consistency throughout the recordings. Both approaches provided robust support for the technical validity of the dataset in the context of blade fault diagnosis in multirotor UAVs.

Classification-based validation using additional experimental data. In the first validation approach, an external test set comprising newly collected vibration signals—generated exclusively under blade damage scenarios involving mass removal—was used. These unseen samples were tested against machine learning classifiers originally trained on the main dataset. The objective was to assess whether the trained models could reliably generalize and correctly identify the same type of faults based on real-world vibrations not present during training. The results were found to be highly consistent with the expected outputs, confirming both the clarity of the measured signals and the strength of the class separability. Notably, the classifier accurately identified all fault instances with minimal false predictions. The classification achieved an accuracy, precision, and recall of 0.91, with a specificity of 0.978 and an area under the ROC curve (AUC) of 0.987 which confirms the reliability of the trained model. These results are visually summarized in Fig. 6, where each classified sample is mapped and annotated.

Frequency-domain comparison of blade conditions. To complement the time-domain and time-frequency validation methods, a frequency-domain analysis was conducted using the Fast Fourier Transform (FFT) on the X-axis vibration signals from all five flight conditions. This transformation enables visualization of the signal energy distribution across frequencies, highlighting the spectral differences caused by blade faults. As illustrated in Fig. 7, the healthy UAV condition presents a relatively uniform low-frequency signature, whereas the damaged and unbalanced blade scenarios exhibit noticeable peaks and variations, indicating fault-induced harmonic content. These spectral characteristics offer an additional diagnostic dimension for future researchers and model developers, supporting more informed preprocessing strategies and feature extraction methods. The figure serves as a visual reference to underscore the separability and richness of the dataset in the frequency domain.

Multi-resolution analysis using discrete wavelet transform. The second validation technique relied on a six-level Discrete Wavelet Transform (DWT) to examine the signal's frequency content and identify any latent noise or inconsistency in the recordings. The Daubechies (db4) wavelet was used for decomposition due to its suitability for vibration signal analysis and effective time-frequency localization. Healthy and damaged blade signals were decomposed across multiple levels to isolate high- and low-frequency components. This analysis enabled evaluation of noise presence, the clarity of signal transitions, and determination of the most suitable decomposition level for feature extraction. The quality of the decomposition was remarkable, and no significant noise distortions were observed across any level, demonstrating the integrity of the original measurements. Additionally, a fusion of selected decomposition levels was tested to simulate hybrid signal processing strategies, which yielded superior signal clarity and class distinctiveness. Calibration of the accelerometer sensor also played a critical role in achieving consistent and artifact-free recordings, ensuring the dataset is ready for further transformation into either frequency-domain or time-frequency domain representations with minimal preprocessing effort. Figure 8 illustrates a side-by-side wavelet decomposition of healthy and damaged blade signals, highlighting the smooth transitions and well-preserved waveform structure across all levels.

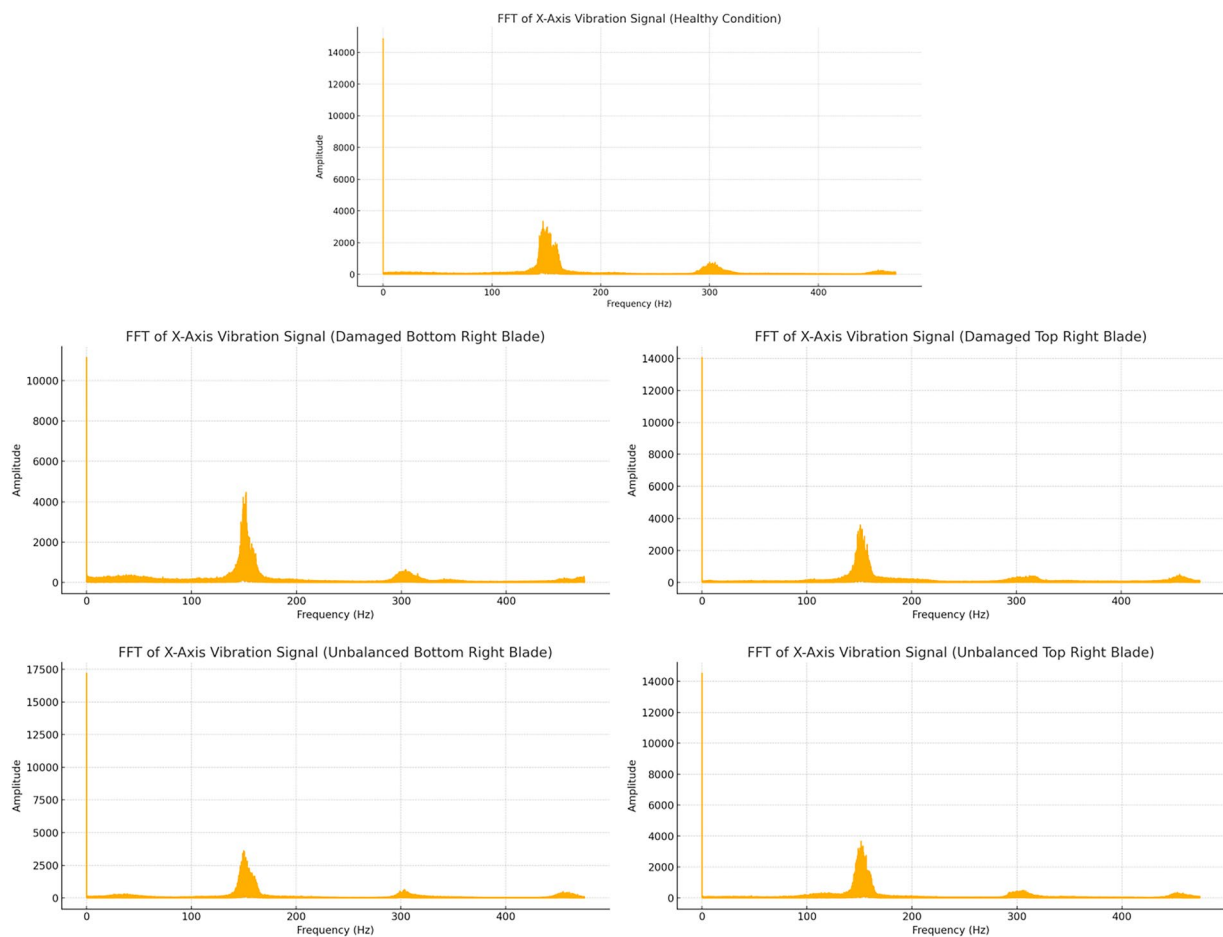


Fig. 7 FFT plots of X-axis vibration signals for all UAV blade conditions, illustrating frequency-domain differences between healthy, damaged, and unbalanced states.

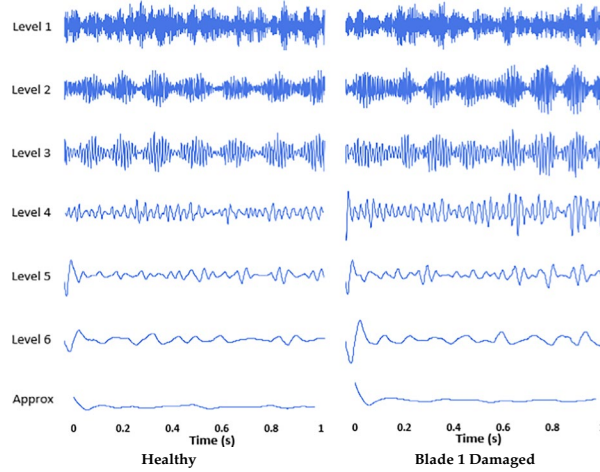


Fig. 8 Six-level wavelet decomposition of vibration signals for healthy vs. damaged blades.

Usage Notes

The dataset is compatible with a variety of ML platforms and can be easily processed using both traditional and deep learning techniques. The current study particularly recommends the use of Orange Data Mining²³, an open-source data visualization and analysis tool, for rapid prototyping of classification pipelines^{24,25}. Orange allows users to create workflow-based data analysis structures with minimal coding experience as it is especially suitable for researchers and educators working in topics of fault diagnosis, specifically UAV fault detection.

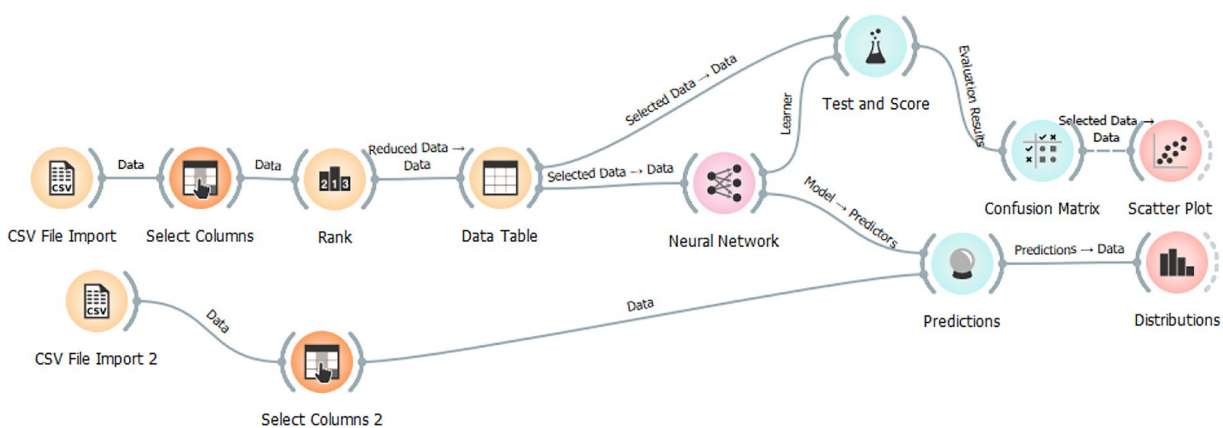


Fig. 9 Orange data mining prediction structural workflow utilizing a simple neural network¹⁰.

Figure 9 illustrates an example Orange workflow used for classification in a previously published study based on this dataset. The visual workflow provides a clear representation of how features were selected, processed, and classified and generally serves as a helpful reference for future reuse and experimentation.

Code availability

No custom code was used to generate or process the dataset described in this manuscript.

Received: 11 April 2025; Accepted: 24 July 2025;

Published online: 07 August 2025

References

1. Yang, Q. *et al.* Prediction of Flight Status of Logistics UAVs Based on an Information Entropy Radial Basis Function Neural Network. *Sensors* **21** (2021).
2. Wang, J., Yang, K., Wu, B. & Wang, J. Cooperative Path Planning for Persistent Surveillance in Large-Scale Environment with UAV-UGV System. *IEEE Transactions on Electrical and Electronic Engineering* **n/a** (2024).
3. Cheng, K. *et al.* Heterogeneous UAV Swarm Collaborative Search Mission Path Optimization Scheme for Dynamic Targets. *International Journal of Aerospace Engineering* **2024**, 6643424 (2024).
4. Huang, C.-H., Chen, Y.-C., Hsu, C.-Y., Yang, J.-Y. & Chang, C.-H. FPGA-based UAV and UGV for search and rescue applications: A case study. *Computers and Electrical Engineering* **119**, 109491 (2024).
5. Ai, S., Song, J., Cai, G. & Zhao, K. Active Fault-Tolerant Control for Quadrotor UAV against Sensor Fault Diagnosed by the Auto Sequential Random Forest. *Aerospace* **9**, 518 (2022).
6. Saeid, M., Lussier, B., Fantoni, I., Shraim, H. & Francis, C. Fault Diagnosis and Fault-Tolerant Control of an Octorotor UAV using motors speeds measurements. *IFAC-PapersOnLine* **50**, 5263–5268 (2017).
7. Iannace, G., Ciaburro, G. & Trematerra, A. Fault diagnosis for UAV blades using artificial neural network. *Robotics* **8**, 59 (2019).
8. Liang, S. *et al.* Data-driven fault diagnosis of FW-UAVs with consideration of multiple operation conditions. *ISA Trans* **126**, 472–485 (2022).
9. Al-Haddad, L. A. *et al.* Protocol for UAV fault diagnosis using signal processing and machine learning. *STAR Protoc* **5** (2024).
10. Al-Haddad, L. A. & Jaber, A. A. An Intelligent Fault Diagnosis Approach for Multirotor UAVs Based on Deep Neural Network of Multi-Resolution Transform Features. *Drones* **7**, 82 (2023).
11. Al-Haddad, L. A. & Jaber, A. A. An Intelligent Quadcopter Unbalance Classification Method Based on Stochastic Gradient Descent Logistic Regression. in *2022 3rd Information Technology To Enhance e-learning and Other Application (IT-ELA)* 152–156, <https://doi.org/10.1109/IT-ELA57378.2022.10107922> (2022).
12. Al-Haddad, L. A. & Jaber, A. A. Improved UAV blade unbalance prediction based on machine learning and ReliefF supreme feature ranking method. *Journal of the Brazilian Society of Mechanical Sciences and Engineering* **45**, 463 (2023).
13. Al-Haddad, L. A., Giernacki, W., Shandookh, A. A., Jaber, A. A. & Puchalski, R. Vibration Signal Processing for Multirotor UAVs Fault Diagnosis: Filtering or Multiresolution Analysis? *Eksplotacja i Niegawodność – Maintenance and Reliability* <https://doi.org/10.17531/ein/176318> (2023).
14. Al-Haddad, L. A. & Jaber, A. A. Influence of Operationally Consumed Propellers on Multirotor UAVs Airworthiness: Finite Element and Experimental Approach. *IEEE Sens J* **1**, <https://doi.org/10.1109/ISEN.2023.3267043> (2023).
15. Al-Haddad, L. A., Jaber, A. A., Neranon, P. & Al-Haddad, S. A. Investigation of Frequency-Domain-Based Vibration Signal Analysis for UAV Unbalance Fault Classification. *Engineering and Technology Journal* **41**, 1–9 (2023).
16. Jaber, A. A. & Al-Haddad, L. A. Integration of Discrete Wavelet and Fast Fourier Transforms for Quadcopter Fault Diagnosis. *Exp Tech* <https://doi.org/10.1007/s40799-024-00702-3> (2024).
17. Kim, T., Kim, S. & Shin, H.-S. Data-driven diagnosis of multicopter thrust fault using supervised learning with inertial sensors. *Journal of Aerospace Information Systems* **20**, 690–701 (2023).
18. Yaman, O., Yol, F. & Altinors, A. A fault detection method based on embedded feature extraction and SVM classification for UAV motors. *Microprocess Microsyst* **94**, 104683 (2022).
19. Baldini, A. *et al.* Real-time propeller fault detection for multirotor drones based on vibration data analysis. *Eng Appl Artif Intell* **123**, 106343 (2023).
20. Sadhu, V., Anjum, K. & Pompili, D. On-board deep-learning-based unmanned aerial vehicle fault cause detection and classification via fpgas. *IEEE Transactions on Robotics* **39**, 3319–3331 (2023).
21. Al-Haddad, L. A. *et al.* Energy consumption and efficiency degradation predictive analysis in unmanned aerial vehicle batteries using deep neural networks. *Advances in Science and Technology Research Journal* **19**, 21–30 (2025).
22. Luttfi, A. Al-Haddad. Dataset on UAV Fault Diagnosis Using Vibrational Signals. *Figshare* <https://doi.org/10.6084/m9.figshare.28765640> (2025).

23. Demšar, J., Zupan, B., Leban, G. & Curk, T. Orange: From Experimental Machine Learning to Interactive Data Mining. in *Knowledge Discovery in Databases: PKDD 2004* (eds. Boulicaut, J.-F., Esposito, F., Giannotti, F. & Pedreschi, D.) 537–539 (Springer Berlin Heidelberg, Berlin, Heidelberg, 2004).
24. Ferhi, W., Hadjila, M., Djillali, D. M. & Bouidaine, A. B. Machine Learning-based Classification of Diabetes Disease: A Case Study with Orange Data Mining. *2023 International Conference on Electrical Engineering and Advanced Technology (ICEEAT)* 1, 1–6 (2023).
25. Tiwari, R., Kumar, G. & Gunjan, V. K. Effect of Environment on Students Performance Through Orange Tool of Data Mining. in *Proceedings of the 4th International Conference on Data Science, Machine Learning and Applications* (eds. Kumar, A., Gunjan, V. K., Hu, Y.-C. & Senatore, S.) 283–292 (Springer Nature Singapore, Singapore, 2023).

Acknowledgements

The authors extend their appreciation to Northern Border University, Saudi Arabia, for supporting this work through project number (NBU-CRP-2025-2484). This research is also partially funded by European Union under the REFRESH—Research Excellence For Region Sustainability and High-Tech Industries Project via the Operational Program Just Transition under Grant CZ.10.03.01/00/22_003/0000048; in part by the National Centre for Energy II and ExPEDite Project a Research and Innovation Action to Support the Implementation of the Climate Neutral and Smart Cities Mission Project TN02000025; and in part by ExPEDite through European Union's Horizon Mission Program under Grant 101139527.

Author contributions

Conceptualization, A.A.J., M.N.H., H.K., M.I.A.-K. and A.F.; methodology, L.A.A.; software, L.A.A.; validation, L.A.A.; formal analysis, L.A.A.; investigation, L.A.A.; writing—original draft preparation, L.A.A.; writing—review and editing, A.A.J., M.N.H., H.K., M.I.A.-K. and A.F. All authors have read and agreed to the published version of the manuscript.

Competing interests

The authors declare no competing interests.

Additional information

Correspondence and requests for materials should be addressed to L.A.A.-H. or H.K.

Reprints and permissions information is available at www.nature.com/reprints.

Publisher's note Springer Nature remains neutral with regard to jurisdictional claims in published maps and institutional affiliations.



Open Access This article is licensed under a Creative Commons Attribution-NonCommercial-NoDerivatives 4.0 International License, which permits any non-commercial use, sharing, distribution and reproduction in any medium or format, as long as you give appropriate credit to the original author(s) and the source, provide a link to the Creative Commons licence, and indicate if you modified the licensed material. You do not have permission under this licence to share adapted material derived from this article or parts of it. The images or other third party material in this article are included in the article's Creative Commons licence, unless indicated otherwise in a credit line to the material. If material is not included in the article's Creative Commons licence and your intended use is not permitted by statutory regulation or exceeds the permitted use, you will need to obtain permission directly from the copyright holder. To view a copy of this licence, visit <http://creativecommons.org/licenses/by-nc-nd/4.0/>.

© The Author(s) 2025